4398–4414 *Nucleic Acids Research, 2023, Vol. 51, No. 9* *Published online 31 March 2023*
https://doi.org/10.1093/nar/gkad236

Flap endonuclease Rad27 cleaves the RNA of R-loop structures to suppress telomere recombination

Chia-Chun Liu[1,†], Hsin-Ru Chan[1,†], Guan-Chin Su[2,†], Yan-Zhu Hsieh[1], Kai-Hang Lei[2], Tomoka Kato[1], Tai-Yuan Yu[3], Yu-wen Kao[1], Tzu-Hao Cheng[4], Peter Chi[2,5,*] and Jing-Jer Lin[1,*]

[1]Institute of Biochemistry and Molecular Biology, National Taiwan University College of Medicine, Taipei, Taiwan, [2]Institute of Biochemical Sciences, National Taiwan University, Taipei, Taiwan, [3]Institute of Biopharmaceutical Sciences, National Yang Ming Chiao Tung University, Taipei, Taiwan, [4]Institute of Biochemistry and Molecular Biology, National Yang Ming Chiao Tung University, Taipei, Taiwan and [5]Institute of Biological Chemistry, Academia Sinica, Taipei, Taiwan

Received December 12, 2022; Revised March 16, 2023; Editorial Decision March 17, 2023; Accepted March 29, 2023

ABSTRACT

The long non-coding telomeric RNA transcript TERRA, in the form of an RNA–DNA duplex, regulates telomere recombination. In a screen for nucleases that affects telomere recombination, mutations in *DNA2*, *EXO1*, *MRE11* and *SAE2* cause severe delay in type II survivor formation, indicating that type II telomere recombination is mediated through a mechanism similar to repairing double-strand breaks. On the other hand, mutation in *RAD27* results in early formation of type II recombination, suggesting that *RAD27* acts as a negative regulator in telomere recombination. *RAD27* encodes a flap endonuclease that plays a role in DNA metabolism, including replication, repair and recombination. We demonstrate that Rad27 suppresses the accumulation of the TERRA-associated R-loop and selectively cleaves TERRA of R-loop and double-flapped structures *in vitro*. Moreover, we show that Rad27 negatively regulates single-stranded C-rich telomeric DNA circles (C-circles) in telomerase-deficient cells, revealing a close correlation between R-loop and C-circles during telomere recombination. These results demonstrate that Rad27 participates in telomere recombination by cleaving TERRA in the context of an R-loop or flapped RNA–DNA duplex, providing mechanistic insight into how Rad27 maintains chromosome stability by restricting the accumulation of the R-loop structure within the genome.

GRAPHICAL ABSTRACT

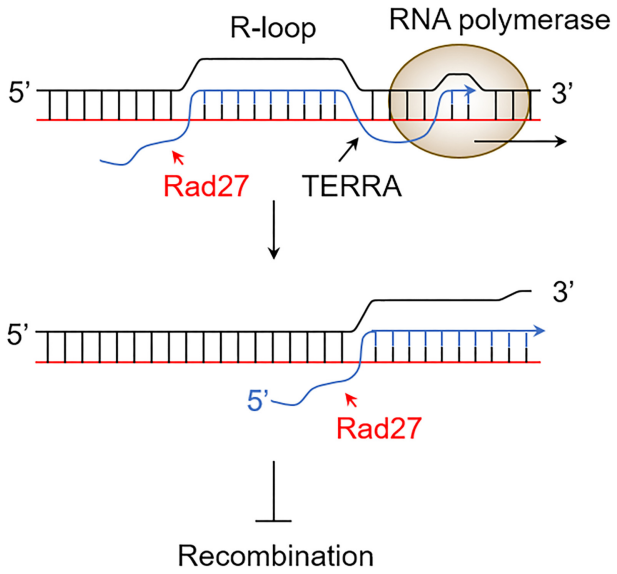

INTRODUCTION

Telomeres are the physical ends of chromosomes, and are crucial for maintaining the stability of chromosomes. In most eukaryotic cells, telomere lengths are maintained by telomerase activity (1). However, cells that lack telomerase rely on a recombination-based mechanism to elongate their telomere DNA (2). Despite the well characterized mechanism of telomere maintenance by telomerase, the molecular details of telomere recombination are not yet clear. In the yeast *Saccharomyces cerevisiae*, telomeres become shorter with each cell division in the absence of telomerase, leading to the uncapping of telomeres and senescence (3,4). A

*To whom correspondence should be addressed. Tel: +886 2 23218823; Fax: +886 2-23915295; Email: jingjerlin@ntu.edu.tw
Correspondence may also be addressed to Peter Chi. Tel: +886 2 23218823; Fax: +886 2 23635038; Email: peterhchi@ntu.edu.tw
†The authors wish it to be known that, in their opinion, the first three authors should be regarded as Joint First Authors.

small population of cells, however, can bypass senescence by activating alternative recombination pathways to maintain their telomeres (5). Two types of *RAD52*-dependent recombination events that contribute to telomere elongation have been identified, generating type I and type II survivors (6–8). Survivor cells generated by these two types of recombination can be distinguished by different growth rates and distinct patterns of their telomeres. Type I survivors result from gene conversion events among the Y′ elements in the subtelomeric regions of chromosomes, and have short terminal telomeric repeats and slow grow rate. In contrast, type II survivors have lengthy and heterogeneous tracts of telomeric DNA repeats, similar to telomeric patterns of the survivors identified in mammalian ALT (alternative lengthening of telomeres) cells (9). These two distinct recombination pathways are genetically defined by *RAD51* and *RAD50*, with type I survivors absent from the *rad51*Δ strain, whereas type II survivors cannot arise from the *rad50*Δ strain (6,10). Budding yeast is considered to be a suitable model for investigating telomerase-independent survival in mammalian cells, since the mechanisms of mammalian ALT and type II recombination are practically indistinguishable.

Despite the identification of important genes involved in regulating telomere recombination, the detailed mechanisms of telomere recombination are not yet fully understood (11). Analysis of mutations in components of the THO complex has revealed the involvement of telomere repeat-containing RNA (TERRA) in type II recombination (12). TERRA is a long non-coding RNA that is transcribed from subtelomeric regions by RNA polymerase II (13). Studies have demonstrated that TERRA stimulates the early formation of type II telomere recombination in telomerase-deficient cells (12,14). Interestingly, TERRA preferentially accumulates on short telomeres due to the degradation of TERRA on long telomeres, which is facilitated by recruitment of the Rat1 nuclease by Rif2 and RNase H2 (15). TERRA association with telomeres facilitates the formation of an RNA–DNA hybrid, which in turn induces telomere recombination. While it is generally considered that the R-loop structure is essential for regulating recombination (12,14), the underlying mechanism by which this RNA–DNA hybrid structure participates in telomere recombination remains to be determined.

To better understand the mechanism underlying type II recombination, we conducted a screening of mutations in nucleases that may affect the R-loop structure. We found that mutations in *dna2*, *exo1*, *mre11* and *sae2* led to severe delays in the formation of type II recombination. Interestingly, mutations in nucleotide excision repair endonucleases, which have been reported to affect ALT formation in mammalian cells (16,17), did not have an impact on telomere recombination in budding yeast. Similarly, mutations in several structure-specific nucleases, such as the *SLX* complex and *HNT3*, which are capable of processing RNA–DNA hybrid structure (18,19), did not appear to alter telomere recombination. Surprisingly, we found that mutations of *YEN1* and *MUS81*, which are the only genes that encode Holliday junction resolvases (20–22), had no effect on type II recombination, suggesting that this process is not mediated through the conventional Holliday junction intermediate. Significantly, mutation in flap endonuclease *RAD27* caused early onset of senescence and type II recombination. Further analysis showed that type II recombination was accompanied by accumulation of telomere-associated RNA–DNA hybrids formed by TERRA and the C-circles. Biochemical analyses showed that Rad27 cleaves the RNA component within an R-loop structure formed *in vitro*, indicating that Rad27 is capable of processing recombination by preventing the accumulation of R-loop structures on telomeres. Thus, we propose that in addition to its well-characterized role in processing Okazaki fragments, Rad27 also plays a crucial role in sustaining chromosome stability by regulating the accumulation of R-loop structures on telomeres.

MATERIALS AND METHODS

Saccharomyces cerevisiae strains and plasmid constructs

The yeast strains used in this study were isogenic to either YPH499 or BY4741. The LiAc/single-strand carrier DNA/PEG transformation method was employed to introduce DNA fragments into yeast cells (23). The *dna2-1* strain was kindly provided by Dr Lorraine Symington (Columbia University, USA). The high-copy plasmid pRS423 was used as the backbone to construct *CUP1* promoter-driven and 3×HA-tagged *TOP1*, *SEN1*, *PIF1* or *RNH1*. Plasmids pET21a-Rad27 and pET21a-Rad27DA were used to express Rad27 and Rad27-DA proteins, respectively, which were generously provided by Dr Yeon-Soo Seo (Korea Advanced Institute of Science and Technology) (24). A DNA fragment comprising the entire *RAD27* open reading frame (ORF) with upstream and downstream 500 bp regions was amplified by polymerase chain reaction (PCR) from yeast genomic DNA using the primers NotI-RAD27p-F (5′-tcagtgGCGGCCGCAAACAAAAAGAACAGGG-3′) and RAD27-3′ UTR-EcoRI-R (5′-tcagtgGAATTCATGGGTTATAATTGTAAGTTG-3′). The amplified *RAD27* fragment was then digested by NotI and EcoRI, and cloned into plasmid pRS316 to generate pRAD27-UTRs (untranslated regions). Mutant plasmid pRAD27-DA-UTRs was generated by replacing the wild-type (WT) *RAD27* of pRAD27-UTRs by the *RAD27-D179A* fragment from pET21a-Rad27DA. Plasmids overexpressing 3×HA-tagged *RAD27* or *rad27-DA* were also generated by subcloning the *RAD27* or *rad27-DA* fragment downstream of a *PGK1* promoter in plasmid pRS426.

Telomere recombination pattern of survivors

The determination of telomere patterns for survivors was previously carried out (10). Briefly, yeast spores from freshly dissected tetrads were grown in liquid medium at 30°C until the cultures reached the stationary phase. The cultures were then diluted ×10 000 and allowed to grow into the stationary phase again. This process was repeated 7–8 times for each strain indicated. Cells from different dilutions were collected, and genomic DNA was digested using a combination of AluI, HaeIII, HinfI and MspI restriction enzymes, fractionated by electrophoresis on 1% agarose gels and analyzed by Southern hybridization with a $C_{1-3}A$ probe.

Determination of senescence rate

The senescence rate was determined in the liquid culture by serial passaging spore products. Colonies grown from dissected tetrads were directly inoculated into liquid media and cultured for 2 days at 25°C. The resulting cultures were then diluted to 3×10^5 cells/ml in fresh medium and cultured for an additional 2 days, with the procedure repeated 8–10 times. Growth rates were measured using a spectrophotometer and converted to population doublings. For senescence analysis on agar plates, cells were harvested directly from freshly dissected *tlc1* spores and assayed by successive re-streaking of grown colonies onto fresh plates 4–6 times. It was estimated that ∼20 population doublings were required for a spore to grow into a colony.

Determination of TERRA in yeast

Yeast cells were grown in selection medium at 30°C. RNA was isolated using the GENEzol TriRNA Pure Kit (Geneaid #GZXD200). Briefly, the cells were resuspended in GENEzol reagent and broken by glass beads. The supernatant was mixed with an equal volume of absolute ethanol, transferred to an RNA-binding (RB) column and centrifuged at 16 000 *g*. DNase I (NEB #M0303) was added to the column matrix and incubated at 30°C for 20 min. The column was washed sequentially with Pre-Wash Buffer and Wash Buffer, and then air-dried. The RNA was eluted with RNase-free water and treated with DNase I at 30°C for 20 min. The RNA was purified using the Geneaid RNA Cleanup Kit (#PR050). To determine TERRA levels, reverse transcription was conducted using oligo$(dT)_{15}$ or $C_{1–3}A$ primer (5′-CCCACCACACACACCCACACCC-3′). Primer pairs for TERRA-1L, 15L, Y′ and *ACT1* have been described previously (15). TERRA and *ACT1* levels were determined by quantitative PCR (qPCR) using the ABI StepOne System.

Determination of RNA–DNA hybrid by immunoprecipitation

To determine the RNA–DNA hybrid formed by TERRA, immunoprecipitation analysis was performed following the previously described protocol (12). Colonies from freshly dissected tetrads were inoculated directly into 10 ml of liquid medium and cultured until the number of cells reached 3×10^8. The cells were resuspended and lysed using the FastPrep-24 system (MP Biomedicals) with phenol/chloroform (pH 8.0) and glass beads. The DNA was then precipitated by ethanol and dissolved in 10 mM Tris–HCl pH 8.0. Then, 100 U of S1 nuclease (Thermo Scientific #EN0321) and 10 μg of RNase A (Thermo Scientific #EN0531) were added to the DNA in the S1 nuclease buffer containing 0.5 M NaCl and incubated at 37°C for 40 min. The reaction was terminated by adding 1 μl of 0.5 M EDTA and 40 μg of proteinase K, and incubating at 50°C for 20 min. The resulting DNA was ethanol precipitated, resuspended in RNase H solution [50 mM Tris–HCl pH 8.3, 75 mM KCl, 5.5 mM $MgCl_2$ and 10 mM dithiothreitol (DTT)], fragmented into ∼500 bp by sonication (Qsonica Sonicator Q700) and then treated with 2 U of RNase III (NEB #M0245). Finally, 10 μg of RNase A and 25 U of RNase H were added in the RNase H + A groups and incubated at 37°C for 16 h.

For the RNA–DNA hybrid immunoprecipitation experiments, DNA was incubated with 20 μl of S9.6 antibody- or IgG-coated Dynabeads Protein G (Invitrogen 10004D) at 4°C for 2 h. The beads were then washed, and DNA was eluted and ethanol precipitated. RNA–DNA hybrid levels were determined by real-time qPCR using the ABI StepOne System. The RNA–DNA hybrid level was calculated using the equation: $2^{\wedge}(Ct_{Input} - Ct_{IP}) \times$ dilution factor.

C-circle assay

To determine the partially double-stranded C-circle DNA, we modified the rolling circle amplification protocol of Henson *et al.* (25). The assay was carried out in a 20 μl reaction mixture consisting of 40 ng of genomic DNA, 4 ng/μl bovine serum albumin (BSA), 0.1% Tween-20, 1 mM each dNTPs and 4 mM DTT. The reaction was initiated with the addition of 7.5 U of ϕ29 DNA polymerase (NEB #M0269) and then incubated at 30°C for 8 h. The reaction was terminated by heating at 70°C for 20 min. Reaction products were diluted with 100 μl of 2× SSC (0.3M NaCl in 30 mM sodium citrate, pH 7.0) and blotted onto a nylon membrane (PerkinElmer #NEF988001PK) using the dot blot apparatus (Bio-Rad). The membrane was then hybridized with either a [γ-^{32}P]ATP-end-labeled or Cy5-end-labeled $C_{1–3}A$ oligonucleotide probe (5′-CCCACCACACACACCCACACCC-3′) at 37°C overnight. The C-circle signal autoradiographs were quantified using Image J software. Plasmid pCT300, carrying ∼300 bp $C_{1–3}A$ telomeric DNA, was used as an internal quantification control.

Protein expression and purification

Escherichia coli Rosetta cells harboring the plasmid expressing *S. cerevisiae* Rad27 WT or Rad27-D179A were cultured in Luria broth at 37°C until the A_{600} reached 0.6–0.8. Isopropyl-β-D-thiogalactopyranoside (IPTG; 1 mM) was added to induce protein expression, and the cells were harvested by centrifugation after a 3 h incubation. All purification steps were carried out at 4°C. To prepare the extract, 30 g of cell paste was suspended in 200 ml of cell breakage buffer [25 mM Tris–HCl, pH 7.5, 10% glycerol, 0.5 mM EDTA, 300 mM KCl, 0.01% Igepal, 1 mM 2-mercaptoethanol, the protease inhibitors aprotinin, chymostatin, leupeptin and pepstatin A at 3 μg/ml each, 1 mM phenylmethylsulfonyl fluoride (PMSF) and benzamidine] and sonicated. After centrifugation (100 000 *g* for 60 min), the clarified lysate was incubated with 3 ml of Ni^{2+} NTA–agarose (Qiagen) for 2 h. The matrix was poured into a column, washed with 50 ml of buffer K (20 mM K_2HPO_4, pH 7.5, 10% glycerol, 0.5 mM EDTA, 0.01% Igepal and 1 mM 2-mercaptoethanol) containing 500 mM KCl and 5 mM imidazole, followed by 25 ml of buffer K containing 300 mM KCl and 20 mM imidazole. Rad27 WT was eluted with 30 ml of 200 mM imidazole in buffer K containing 300 mM KCl. The fractions containing Rad27 WT were dialyzed by buffer K containing 50 mM KCl for 1 h. The sample was then fractionated in a 1 ml Macrohydroxyapatite

(Bio-Rad) column, using a 60 ml gradient of 0–490 mM KH_2PO_4 in buffer K. Fractions containing the Rad27 WT peak were further fractionated in a 1 ml Source S column, using a 30 ml gradient of 97.5–1000 mM KCl in buffer K. The fractions containing Rad27 WT were pooled and concentrated to 10–20 mg/ml in a Centricon-10 concentrator. The concentrated proteins were divided into small aliquots and stored at –80°C. Rad27-D179A was purified using the same procedure as for the WT protein.

Preparation of R-loop and double-flap substrates

The oligonucleotide sequences used in this study are presented in Supplementary Table S1. To prepare the substrates, RNA oligo 1 was labeled with [γ-^{32}P]ATP (PerkinElmer Life Sciences) using T4 polynucleotide kinase (New England Biolabs). Radiolabeled RNA oligo 1 was then separated from free [γ-^{32}P]ATP using a Bio-Spin 6 column (Bio-Rad). For the R-loop substrate, the radiolabeled RNA oligo 1 was annealed to oligo 2 by heating to 65°C and slow cooling to room temperature in annealing buffer (50 mM Tris–HCl pH 7.5, 10 mM $MgCl_2$, 100 mM NaCl and 1 mM DTT). The RNA–DNA hybrid was then annealed to oligo 3 by heating to 55°C and slowly cooling to room temperature in the annealing buffer. The annealed substrates were separated on a 10% native polyacrylamide gel in 1× TBE buffer (89 mM Tris, 89 mM borate, 2 mM EDTA, pH 8.0) at 4°C. The gel band corresponding to the annealed substrates was excised, and the substrates were eluted from the gel by polyacrylamide gel electrophoresis (PAGE) in 1× TBE buffer at 4°C. The eluted substrates were further concentrated using a Centricon-10 concentrator and were ready to use for *in vitro* assays or storage at –20°C. For the double-flap substrates, radiolabeled RNA was annealed to oligo 4. The RNA–DNA hybrid was then annealed to oligo 3 (for a 76 nt double-flap) or oligo 5 (for a 1 nt double-flap) as described above. Validation of the annealed substrates was confirmed by treatment with BamHI, EcoRI or RNase H.

The analysis of substrate cleavage by Rad27

The specified amount of purified Rad27 WT or D179A mutant was incubated with the indicated substrates in buffer A (25 mM Tris–HCl pH 7.5, 1 mM DTT, 2 mM $MgCl_2$, 80 ng/μl BSA, 20 mM KCl). The reactions were then incubated at 30°C for the indicated time and stopped by addition of proteinase K (1 mg/ml) and sodium dodecylsulfate (SDS; 0.005% final concentration) at 37°C for 10 min. The reaction mixtures were resolved on a 10% native polyacrylamide gel in 1× TBE buffer at 4°C. After the gel was dried onto DE81 paper (Whatman), radiolabeled species in the dried gel were analyzed by phosphorimaging in a Personal Molecular Imager (Bio-Rad) using Quantity One software (Bio-Rad).

RESULTS

Disruption of the R-loop structure delayed telomere recombination

Previously, it was found that TERRA could induce telomere recombination at telomeres by forming RNA–DNA hybrids (12,14,26). However, the specific role of the R-loop structure in telomere recombination was unclear. In this study, we evaluated the effects of genes known to regulate the formation of the R-loop structure during telomere recombination in yeast cells. *RNH1* encodes RNase H1, which degrades the RNA moiety from the RNA–DNA duplex. *TOP1* encodes a type IB topoisomerase that removes both negative and positive supercoiled DNAs formed after transcription, preventing the formation of the R-loop structure (27). *SEN1* encodes an ATP-dependent 5′ to 3′ RNA–DNA and DNA helicase, which is a component of the exosome-associated nuclear pre-mRNA down-regulation (NRD) complex (28,29). It restricts the occurrence of RNA–DNA hybrids that might form during transcription. *PIF1* encodes an ATP-dependent 5′ to 3′ helicase that prefers to unwind the RNA–DNA duplex (30,31). It plays a significant role in removing the telomerase from telomeres (32). Based on our hypothesis that the R-loop structure is necessary for telomere recombination, we anticipated that an excessive amount of these proteins would remove the R-loop structure and prevent telomere recombination.

Plasmids carrying *RNH1*, *TOP1*, *SEN1* or *PIF1* were introduced and overexpressed in telomerase-deleted (*tlc1*) yeast cells to assess their effects on telomere recombination (Figure 1A). Cells containing these plasmids were collected directly from freshly dissected *tlc1* spores and analyzed. Southern blot analysis was used to assess telomere recombination in the survivors obtained from liquid cultures after successive dilutions (7,10). In *tlc1* cells, the type II survivor pattern was mostly observed between the fourth and fifth dilutions (Figure 1B). However, in *tlc1* cells overexpressing *RNH1*, *TOP1*, *SEN1* or *PIF1* genes, the conversion of the type I to the type II recombination pattern was significantly delayed (Figure 1B). These results suggest that an R-loop structure formed by TERRA may be critical for telomere recombination, as an excessive amount of RNase H, topoisomerase or helicases Sen1 or Pif1 delays type II recombination.

Screening for yeast nucleases that regulate type II telomere recombination

We next investigated how the R-loop structure facilitates the initiation of telomere recombination. Since the R-loop structure is critical for this process, we hypothesized that nucleases involved in regulating R-loop formation should also participate in telomere recombination. Using the *Saccharomyces* genome database (https://www.yeastgenome.org/), we identified 104 nucleases that encode or associate with nuclease activities. We excluded 43 transposon nucleases, the HO endonuclease and Spo11 (due to their well-documented function in mating-type switch and meiosis, respectively), nucleases within DNA polymerases (*POL2*, *POL3* and *POL32*), nucleases located within organelles, including mitochondria and vacuoles, and nucleases whose mutations cause lethality. For comparison, we included four mitochondria nucleases (*DSS1*, *LCL3*, *NGL1* and *REX2*) and one vacuole nuclease (*RNY1*) as non-nuclear nucleases in the analysis. As a result, we selected a total of 44 nucleases to examine their influence on telomere recombination (Table 1). To determine whether these nucleases are involved

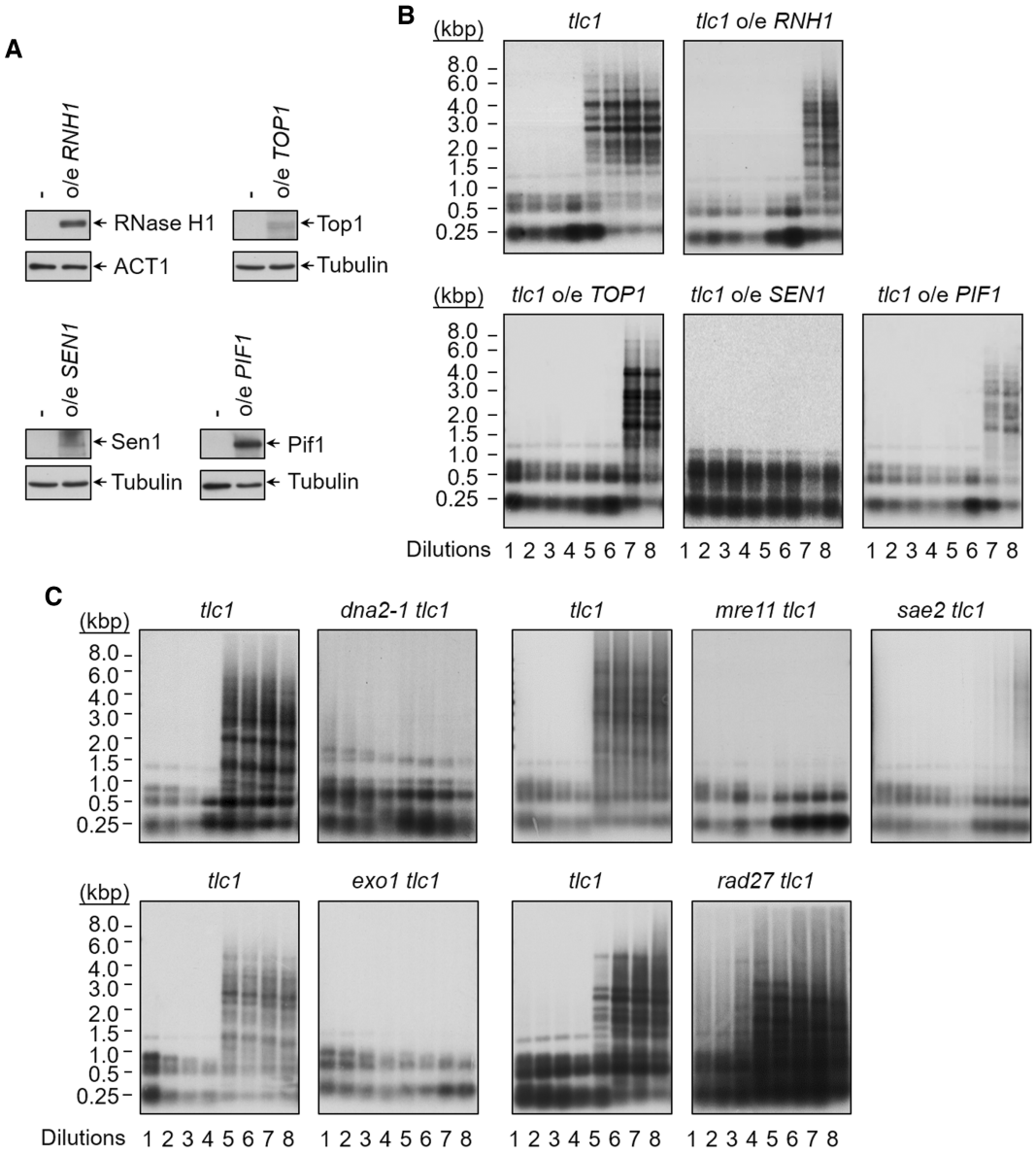

Figure 1. Identification of nucleases that affect type II telomere formation. (**A**) Immunoblots of *RNH1*, *TOP1*, *SEN1* or *PIF1* overexpression in *tlc1* cells. (**B**) Delayed type II survivor formation in *tlc1* cells overexpressing *RNH1*, *TOP1*, *SEN1* or *PIF1*. Colonies from freshly dissected tetrads were inoculated directly into liquid YEPD medium and cultured at 30°C until reaching stationary phase. The cultures were diluted 1:10 000 into fresh medium and cultured at 30°C for seven repeats. Genomic DNA was extracted and digested using a combination of AluI, HaeIII, HinfI and MspI. Southern blot analyses were conducted using a $C_{1-3}A$ probe. (**C**) Mutations of selected genes affect type II telomere recombination. Colonies from the indicated strains were inoculated into liquid YEPD medium and analyzed as described above.

in telomere recombination, we deleted the telomerase RNA component-encoding gene, *TLC1*, in diploid cells harboring each nuclease gene mutation. The nuclease-deleted cells were then collected from freshly dissected *tlc1* spores and assayed by successively diluting the grown cultures into fresh medium eight times. Telomeres of these cultures were analyzed by Southern blotting assays.

Most of the genes tested had negligible effects on telomere recombination, and mitochondrial and vacuole genes did not affect telomere recombination (Supplementary Figure S1; Table 1). Mutations in *CCR4* and *XRN1* showed penetrance effects on telomere recombination (Supplementary Figure S1b, bb). In a total of 10 spores tested, half showed a significant delay in type II survivor formation, while telomere recombination was not affected in the others. This phenotype suggests that despite their involvement in type II recombination, these genes are dispensable in the process of telomere recombination. Notably, mutations in *DNA2*, *EXO1*, *MRE11* and *SAE2* caused a severe delay in type II telomere recombination formation, indicating their essential role in this process (Figure 1C). These results are consistent with prior reports that nuclease *EXO1* and *MRE11/RAD50* are required for type II telomere recombination (10,33–35). Interestingly, the mutation in *RAD27* caused early type II recombination formation (Figure 1C), suggesting that it might negatively regulate telomere recom-

Table 1. Effects of nucleases on telomere recombination[a]

	Gene	Mutant	Property	Type II	Note
1)	*APN1*	*apn1*	AP endonuclease	–	This study
2)	*APN2*	*apn2*	AP endonuclease	–	This study
		apn1 apn2		Slight delay[b]	This study
3)	*CCR4*	*ccr4*	Poly(A) deadenylase	50/50[c]	This study
4)	*DNA2*	*dna2-1*	5′ Flap endonuclease	Delay	This study
5)	*DOM34*	*dom34*	RNA cleavage	–	This study
6)	*DSS1*	*dss1*	Mitochondrial exoribonuclease	–	This study
7)	*DXO1*	*dxo1*	5′–3′ exoRNase activity	–	This study
8)	*EXO1*	*exo1*	5′ Exonuclease	Delay	This study[d,e]
9)	*HNT3*	*hnt3*	5′ AMP hydrolase	–	This study
10)	*IRE1*	*ire1*	ER endoribonuclease	–	This study
11)	*LCL3*	*lcl3*	Mitochondrial nuclease (?)	–	This study
12)	*MKT1*	*mkt1*	Cytoplasmic nuclease	–	This study
13)	*MMS4*	*mus81*	3′ Flap endonuclease	–	This study
14)	*MRE11*	*mre11*	MRX complex	Delay	This study[f]
15)	*MUS81*	*mus81*	Holliday junction resolvase	–	This study
16)	*NGL1*	*ngl1*	Mitochondrial endonuclease	–	This study
17)	*NGL2*	*ngl2*	5.8S rRNA processing	–	This study
18)	*NGL3*	*ngl3*	Poly(A) exonuclease	–	This study
19)	*NTG1*	*ntg1*	AP lyase	–	This study
20)	*NTG2*	*ntg2*	AP lyase	–	This study
		ntg1 ntg2		Lethal	This study
21)	*PAN2*	*pan2*	Poly(A) ribonuclease	–	This study
22)	*POP2*	*pop2*	Poly(A) deadenylase	–	This study
23)	*PSO2*	*pso2*	Nuclease for DNA break repair	–	This study
24)	*RAD1*	*rad1*	NER nuclease	–	This study
25)	*RAD2*	*rad2*	NER nuclease	–	This study
		rad1 rad2		–	This study
26)	*RAD10*	*rad10*	NER nuclease	Slight delay	This study
27)	*RAD17*	*rad17*	NER nuclease	Slight delay	This study
28)	*RAD27*	*rad27*	5′ Flap endonuclease	Early	This study[g]
		rad27 dna2-1		Lethal	This study
29)	*RAI1*	*rai1*	Decapping endonuclease	–	This study
30)	*REX2*	*rex2*	Mitochondrial RNA exonuclease	–	This study
31)	*REX3*	*rex3*	RNA exonuclease	Slight delay	This study
32)	*REX4*	*rex4*	RNA exonuclease (?)	–	This study
33)	*RNH1*	*rnh1*	RNase H1	–	[h]
34)	*RNH201*	*rnh201*	RNase H2	–	[h]
35)	*RNH70*	*rnh70*	Exoribonuclease	–	This study
36)	*RNY1*	*rny1*	Vacuole RNase	–	This study
37)	*RRP6*	*rrp6*	Exosome exonuclease	–	This study
38)	*SAE2*	*sae2*	Structure-specific nuclease	Delay	This study
	rad27 sae2			Lethal	This study
39)	*SLX1*	*slx1*	Structure-specific nuclease	–	This study
40)	*SWT1*	*swt1*	Endoribonuclease	–	This study
41)	*TOP1*	*top1*	Topoisomerase	–	This study
42)	*XRN1*	*xrn1*	Exoribonuclease	50/50	This study
43)	*YBL055C*	*ybl055c*	Nuclease (?)	–	This study
44)	*YEN1*	*yen1*	Holliday junction resolvase	–	This study

[a]All the analyses were conducted in *tlc1* cell; [b]delay type II formation by one dilution; [c]approximately 50% of the colonies showed the delay phenotype (10 colonies were analyzed); [d]Maringele and Lydall (35); [e]Bertuch and Lundblad (33); [f]Teng *et al*. (10); [g]Saharia and Steward (81); [h]Yu *et al*. (12).

bination. Together, the screen identified a specific group of nucleases, including Dna2, Exo1, Mre11, Sae2 and Rad27, involved in regulating telomere recombination.

Notably, mutations in nucleotide excision repair endonuclease genes *RAD1* and/or *RAD2* did not appear to affect telomere recombination (Supplementary Figure S1o). We also analyzed three additional nucleotide excision repair genes, *RAD10*, *RAD14* and *RAD17*, and found that none of them greatly affects type II telomere recombination (Supplementary Figure S1p–r). Thus, although mammalian nucleotide excision repair nucleases XPF and XPG have been reported to be involved in processing R-loop structures (16,17,36), the yeast nucleotide excision repair enzymes were not essential for telomere recombination. Though mutations in the base-excision repair nucleases (Apn1 and Apn2) and AP lyases (Ntg1 and Ntg2) also did not affect telomere recombination (Supplementary Figure S1a, k), the *apn1 apn2* double mutant caused a modest delay in type II survivor formation (Supplementary Figure S1a), suggesting that Apn1 and Apn2 might function redundantly to modulate telomere recombination. Additionally, we show that the 5′ AMP hydrolase *HNT3* (aprataxin deadenylase, APTX in mammals and *Schizosaccharomyces pombe*), which resolves the RNA–DNA junction (18), did

not affect telomere recombination (Supplementary Figure S1f). It was reported that Slx4 is required for resolving the recombination intermediate in ALT cells (19). Slx1 functions as a structure-specific nuclease with Slx4 (37,38). Here, we found that deletion of *SLX1* did not affect type II telomere recombination in yeast (Supplementary Figure S1y).

Holliday junction resolvases are dispensable for type II telomere recombination

Yen1 and Mus81 are the two Holliday junction resolvases identified in yeast (20–22). The screen showed that deletion of either *YEN1* or *MUS81* did not have a significant effect on telomere recombination (Supplementary Figure S1i, S1dd). To determine if they have redundant function in processing Holliday junction during recombination, *mus81 yen1 tlc1* cells were generated. Typically, *tlc1* cells lost viability between the second and third streak on agar plates, and the survivors emerged in the fourth streak (Figure 2A). *mus81 yen1 tlc1* cells appeared sick and grew slowly on agar plates. Survivors of *mus81 yen1 tlc1* cells appeared after five serial streaks. The effects of *mus81 yen1* mutations on the viability of *tlc1* cells were further measured using liquid culture assays (8). The *tlc1*, *mus81 tlc1*, and *yen1 tlc1* cells had reduced growth rate, and survivors were generated after 6–7 days (Figure 2B). The *mus81 yen1 tlc1* cells grew slowly, senesced early and retained a senescent state for ∼7–8 days. Survivors eventually emerged with suboptimal growth phenotype (Figure 2B). Plotting the senescent growth curve as a function of cell divisions showed that survivors of *mus81 yen1 tlc1* cells formed after ∼70 divisions, similar to those observed in *tlc1*, *yen1 tlc1*, or *mus81 tlc1* cells (Figure 2C). These results suggest that although *mus81 yen1 tlc1* cells have defective growth and an extended time for survivor formation, their ability to generate survivors is unaffected.

Telomere length analysis indicated that deletion of *YEN1*, *MUS81* or both did not affect telomere length (Figure 2D, left panel). To investigate whether the defective growth observed in *mus81 yen1 tlc1* cells was due to accelerated telomere shortening, telomere length was measured. Genomic DNA samples were prepared from colonies that had been streaked three times from freshly dissected spores, and telomere lengths were analyzed. The telomere shortening rates in *tlc1*, *yen1 tlc1*, *mus81 tlc1* and *mus81 yen1 tlc1* cells were similar, indicating that the early onset of senescence was not due to accelerated telomere shortening (Figure 2D, right panel). Since the mutants had reduced viability and plating efficiency (Figure 2E), the early onset of senescence is probably due to reduced viability in *mus81 yen1 tlc1* cells. The telomere patterns of survivors were then analyzed, and the *mus81 yen1 tlc1* survivors exhibited the typical type II telomere recombination pattern (Figure 2F). In summary, although the Holliday junction resolvases Yen1 and Mus81 are important for cell viability, they are not required for type II telomere recombination.

Suppression of type II recombination by Rad27 in cells lacking telomerase

Of all the nucleases examined, only the deletion of *RAD27* resulted in the early formation of type II recombination (Figure 1C). *RAD27* is the yeast homolog of mammalian FEN1 flap endonuclease, which is involved in various aspects of DNA metabolism, including replication, repair and recombination (39,40). One of its essential functions is processing Okazaki fragments during lagging strand DNA synthesis. To determine the role of *RAD27* in telomere recombination, we examined the growth of *tlc1* cells carrying *rad27*. Immediately after sporulation, *rad27 tlc1* cells grew more slowly than *tlc1* cells and exhibited severe growth defects on the second streak (Figure 3A). Survivors that bypassed senescence first appeared at the third streak. Using liquid culture assays, *tlc1* cells showed a decline in growth rate, with survivors generated after ∼60–70 generations (Figure 3B). In contrast, although the *rad27 tlc1* mutant had defective growth, survivors were generated after ∼40–50 generations. These results indicate that *RAD27* contributes to senescence and modulates survivor generation in the absence of telomerase.

To determine if the early formation of type II survivors was due to accelerated telomere shortening, the telomere lengths of *rad27* and *rad27 tlc1* cells were analyzed. Freshly dissected *tlc1* spores were streaked onto fresh plates and cells were harvested for telomere length analysis. As shown in Figure 3C, telomere lengths in *rad27* cells were similar to those in WT cells, indicating that *RAD27* did not play a role in telomere length maintenance. Additionally, deleting *RAD27* in *tlc1* cells did not significantly alter telomere shortening rates, suggesting that the early senescence and formation of type II recombination in *rad27 tlc1* cells were not caused by an increased overall telomere erosion rate. This analysis was limited to the first two streaks of *rad27 tlc1* cells, as the type II recombination pattern appeared early in these cells. To further investigate the effect of *rad27* on survivor types, genomic DNAs from survivors of *tlc1* and *rad27 tlc1* strains were analyzed (10). As shown in Figure 3D, in contrast to the ∼80–90% of type I survivors observed in *tlc1* cells, the deletion of *RAD27* in cells resulted in a significantly higher formation of type II survivors. These results suggest that *RAD27* is critical for suppressing type II recombination in cells lacking telomerase.

Flap endonuclease activity of Rad27 is required to suppress telomere recombination

To investigate the requirement for flap endonuclease activity of Rad27 in suppressing telomere recombination, a nuclease-inactive *rad27-DA* mutant was generated by replacing the Asp179 residue with Ala (24). Centromeric plasmid (pRS316) carrying the WT or the *rad27-DA* mutant was introduced into *rad27 tlc1* cells, and the results showed that only WT *RAD27* rescued the formation of early survivors, while the *rad27-DA* mutant showed similar survival patterns to the vector control (Figure 3E). Next, we examined whether the Rad27 nuclease activity is necessary for telomere recombination suppression. In line with the requirement for cell growth, flap endonuclease activity was necessary for suppressing type II telomere recombination in *rad27 tlc1* cells (Figure 3F). It is also noteworthy that the expression of *rad27-DA* inhibited cell growth and promoted telomere recombination in *rad27 tlc1* cells. To determine whether excess Rad27 can suppress type II recombination, a high copy

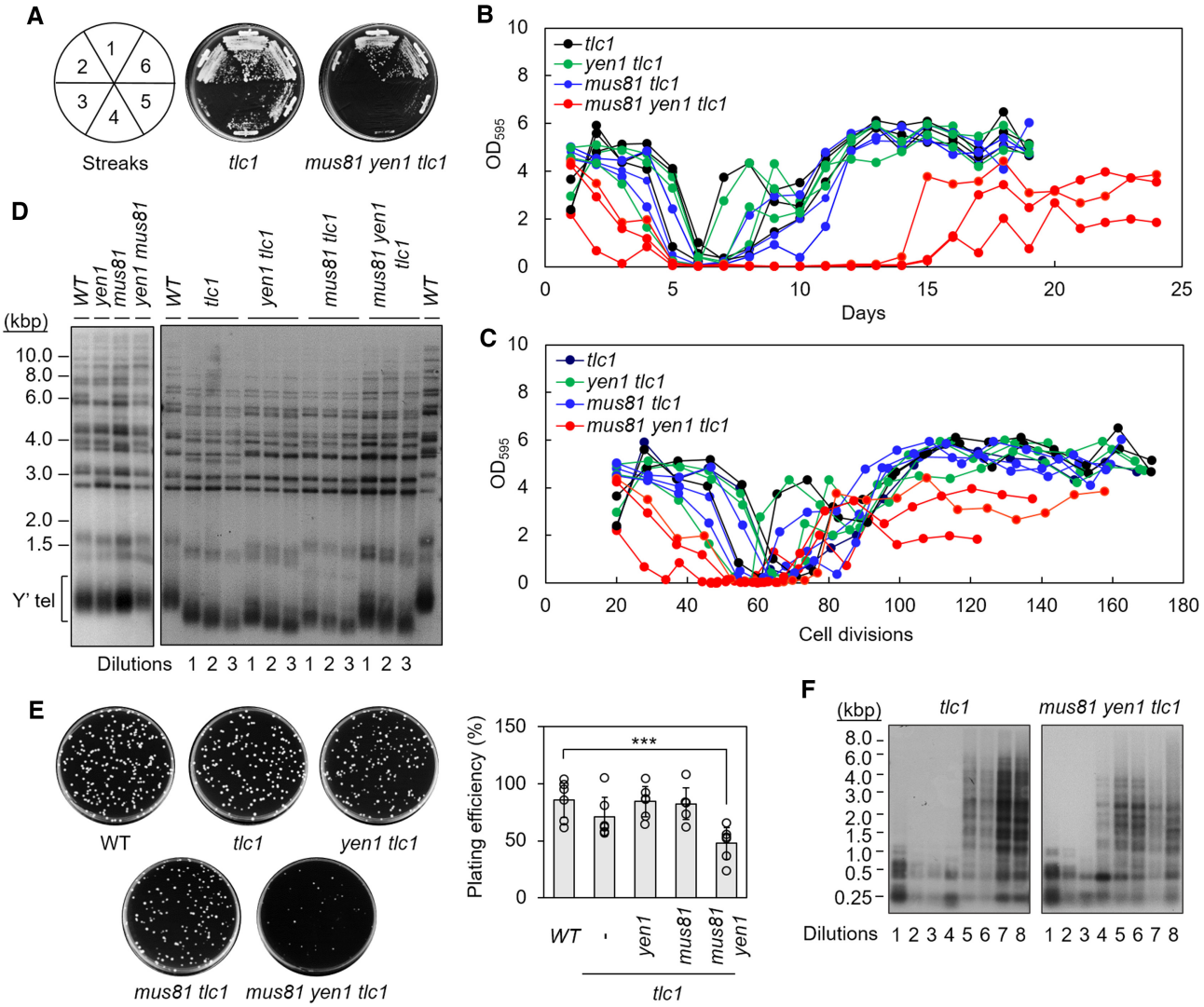

Figure 2. Holliday junction resolvases do not affect type II survivor formation. (**A**) Early senescence induced by *mus81 yen1* in *tlc1* cells. Colonies from freshly dissected tetrads were continually streaked on YEPD plates at 30°C six successive times (first to sixth streaks). Photographs of these cells from the first to sixth streaks on YEPD plates are presented. (**B**) Colonies from freshly dissected tetrads were inoculated directly into liquid YEPD medium at a concentration of 3×10^5 cells/ml and cultured at 25°C for 1 day. The cultures were diluted to the same concentration and cultured at 25°C for another day. These procedures were repeated until survivors formed. Results of three independent colonies from each strain are presented. Cell growth was measured by a spectrophotometer. (**C**) Data from (B) presented as a function of cell divisions. (**D**) Mutations of *YEN1* and/or *MUS81* did not affect the telomere erosion rates in telomerase-deficient cells. DNA was isolated from cells that had undergone one, two or three successive streaks, digested with XhoI, separated on a 1% agarose gel and analyzed by Southern blotting using a $C_{1-3}A$ probe. (**E**) Decreased colony forming ability in *mus81 yen1 tlc1* cells. Colonies from freshly dissected tetrads were selected, resuspended in water, and ∼300 cells were plated directly onto YEPD plates and incubated at 30°C. The number of colonies formed was counted, and plating efficiencies were determined as the number of colonies divided by 300. Results were obtained from averages of six independent experiments, and *P*-values were determined by two-tailed unpaired *t*-test. ***$P < 0.001$. (**F**) *MUS81* and *YEN1* did not affect type II telomere recombination. As in Figure 1B, DNAs prepared from *tlc1* and *mus81 yen1 tlc1* cells were analyzed by Southern blotting.

plasmid (pRS426) carrying *RAD27* was introduced into *tlc1* cells. We found that overexpressing *RAD27* did not affect the timing of survivor formation and the type II recombination pattern in *tlc1* cells (Supplementary Figure S2). Since the estimated Rad27 level in cells is ∼1400–6100 molecules (41,42), additional Rad27 might not further suppress telomere recombination.

Overexpression of *EXO1* or *DNA2* is known to alleviate the phenotypes associated with *rad27*, such as temperature sensitivity and elevated mutation frequency, which are related to its involvement in DNA replication (43–45). Exo1 has both 5′–3′ exonuclease and flap endonuclease activities (46,47), while Dna2 carries a DNA-dependent helicase and 5′ flap endonuclease activity, which is essential for DNA replication (48–50). We investigated whether the structure-specific nuclease activities of these two enzymes can suppress telomere recombination phenotypes of *rad27*, since the 5′ flap endonuclease activity of Rad27 is required for suppressing telomere recombination. We analyzed the effects of overexpressing *EXO1* or *DNA2* on senescence and telomere recombination (Supplementary Figure S3). The results showed that overexpression of *EXO1* partially re-

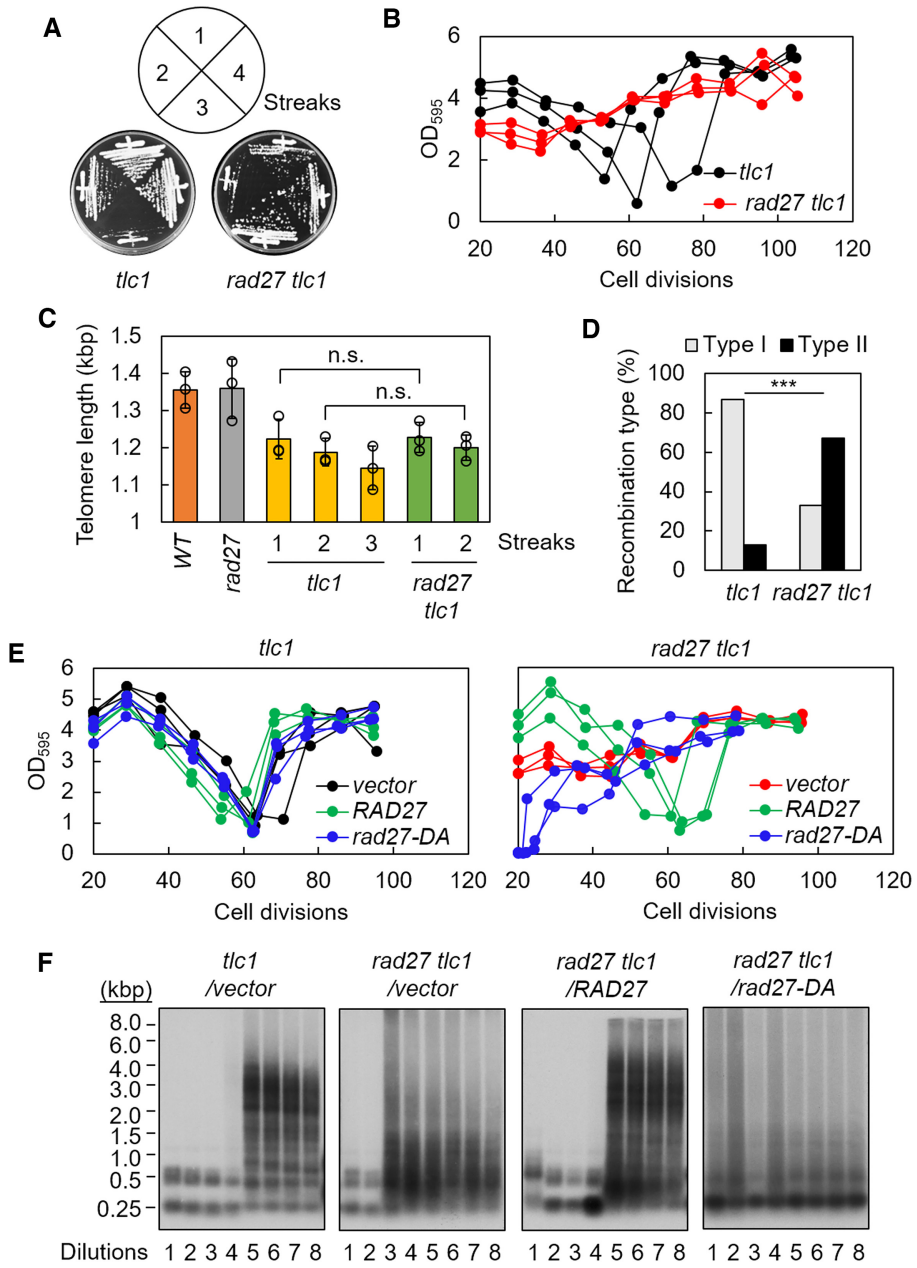

Figure 3. Nuclease activity of Rad27 is required for suppressing type II telomere recombination. (**A**) Induction of early senescence by *rad27* in *tlc1* cells. As described above, colonies from freshly dissected tetrads were streaked on YEPD plates at 30°C four times (first to fourth streaks). Photographs of these cells from each streak are presented. (**B**) Senescence curves were analyzed for *tlc1* and *rad27 tlc1* cells as described in Figure 2C. (**C**) Mutation of *RAD27* did not affect the rate of telomere length erosion in telomerase-deficient cells. DNA was isolated from WT, *rad27*, *tlc1* and *rad27 tlc1* cells that had undergone one, two or three streaks, digested with XhoI, separated on a 1% agarose gel, and analyzed by Southern blotting using a $C_{1–3}A$ probe. The lengths of Y′ telomeres were quantified and plotted. The results show the mean and standard deviation (SD) of three independent experiments. (**D**) *rad27 tlc1* cells showed an increased frequency of type II survivor formation relative to *tlc1* cells. Genomic DNA from 15 independent survivors from each strain was isolated, digested with four enzymes and analyzed by Southern blotting with a $C_{1–3}A$ probe. The percentages of survivors were quantified. The *P*-value was determined by a χ^2 test. ***$P < 0.001$. (**E**) Senescence curves were analyzed for *tlc1 cells* or *rad27 tlc1* cells with or without addition of *RAD27* or *rad27-DA* as described in Figure 2C. (**F**) Type II telomere recombination was analyzed in the indicated cells harboring *RAD27* or *rad27-DA*.

stored the timing of survivor formation and the type II recombination pattern in *rad27 tlc1* cells. In comparison, overexpression of *EXO1* did not have a significant impact on either survivors or telomere recombination in *tlc1* cells. Similarly, *DNA2* did not affect the formation of survivors or telomere recombination. Thus, although overexpression of *EXO1* or *DNA2* can alleviate replication defects in *rad27* cells, neither enzyme can completely replace the distinct function of *RAD27* in telomere maintenance.

Cleavage of TERRA RNA on the R-loop structure by Rad27

After establishing the role of TERRA in telomere recombination, a quantitative real-time reverse transcription–PCR (RT–PCR) assay was conducted to measure TERRA levels in yeast cells lacking *RAD27* (12,51). In *S. cerevisiae*, subtelomeric Y′ elements are often found next to the repeated $TG_{1–3}$ telomeric sequences. Here, we focused on analyzing TERRA of chromosomes 1L (TERRA-1L), 15L (TERRA-15L) and the Y′ elements (TERRA-Y′). As shown in Figure 4A, introduction of *rad27* in *tlc1* cells resulted in a significant increase in TERRA-1L, 15L and TERRA-Y′ levels. However, the restoration of *RAD27* led to a decrease in TERRAs, indicating that *RAD27* suppresses their abundance. The level of TERRA in the form of RNA–DNA hybrids was further analyzed using direct immunoprecipitation analysis with the S9.6 antibody (52) on DNA samples prepared through a neutral phenol extraction, which preserves the DNA-associated RNA. The *rad27 tlc1* cells had higher levels of telomere-associated TERRA on 1L, 15L and Y′ telomeres compared with *tlc1* and *rad27* cells (Figure 4B). These elevated TERRA levels were sensitive to RNase H digestion and reduced by expressing *RAD27*, indicating that these TERRAs are indeed telomere associated and *RAD27* dependent. Thus, the results suggest that *RAD27* is involved in suppressing the accumulation and formation of telomere-associated TERRA. Note that RNase A was included in addition to RNase H in the experiments presented in Figure 4B to eliminate TERRA from RNA–DNA hybrids. The combined use of both enzymes effectively reduces the levels of telomere-associated TERRA in these experiments (Supplementary Figure S4).

With the suppressive function of *RAD27* in type II recombination, Rad27 seemingly utilizes its flap endonuclease activity to process the R-loop structure. To test this hypothesis, recombinant WT Rad27 and its nuclease-dead D179A mutant proteins were expressed and purified from *E. coli.* Their abilities to cleave the R-loop structure were then assessed (Figure 5A). A nucleic acid substrate that mimics the R-loop structure was prepared for the analysis (Figure 5B; Supplementary Figure S5). This R-loop structure was assembled using two DNA molecules and one RNA molecule, which were triple-labeled with two DNA strands labeled by Cy3 and Cy5, respectively, and radiolabeled RNA. As shown in Figure 5C, the assembled R-loop structure was cleaved by the built-in cutting sites of EcoRI and BamHI, and the RNA portion was sensitive to RNase H digestion, suggesting that the reconstituted molecule was comparable with an R-loop structure.

The reconstituted R-loop structure formed by TERRA was incubated with purified Rad27 and analyzed. As shown in Figure 5D, two distinct cleavage products were observed on the RNA component of the R-loop in an Rad27 dose-dependent manner, while the DNA components of the R-loop structure remained intact (Figure 5D, middle and right panels). The major and minor cleavage products were 6 and 8 nt, respectively, from the 5′ end of the RNA molecule. Titration of Rad27 showed that cleavage of TERRA RNA was highly effective, as nearly 90% of the substrate was cleaved at low Rad27 concentrations within 15 min (Figure 5D–F). The activity of Rad27 is essential for the cleavage of TERRA RNA since the catalytically defective D179A mutant (Rad27-DA) was unable to generate detectable cleavage products (Figure 5D–F). These results clearly indicate that Rad27 can cleave the RNA component of the R-loop structure.

As RNA polymerase II may quickly reach the end of the DNA and run off the telomeres following transcription of TERRA, the R-loop structure may convert to a double-flap RNA–DNA hybrid structure. To test whether the double-flap structure was also a suitable substrate for Rad27, two double-flap substrates carrying either a 1 nt or a 76 nt tail were synthesized, respectively (Supplementary Figure S5), and compared with the R-loop structure for their cleavage by Rad27. As shown in Figure 5G, Rad27 efficiently cleaved both the R-loop and double-flap structures, with a preference for cleaving the R-loop structure over the short or long double-flap structure under the same experimental conditions. Notably, Rad27 did not cleave TERRA RNA when it lacked an R-loop or double-flap structure (Supplementary Figure S6). It is also noteworthy that a 16mer product was generated by Rad27 on a short double-flap substrate, consistent with the predicted site of Rad27 that cleaves one nucleotide into the annealed region (53). In contrast, the 6mer and 8mer products were the primary products when the R-loop or long double-flap substrate was cleaved by Rad27. However, the mechanism by which Rad27 generates distinct sizes of RNA fragments on the R-loop and long double-flapped substrates remains unclear. Taken together, these findings suggest that TERRA RNAs on R-loop and double-flap structures are preferred substrates for Rad27.

Generation of extrachromosomal C-circles in *rad27* cells

Yeast type II recombinants have telomeres similar to mammalian ALT cells (54), suggesting a potential shared mechanism of generation. In both human ALT cells and survivors of telomerase-deficient yeast cells, extrachromosomal telomeric DNA fragments, particularly single-stranded C-rich circles, are commonly found (25,55–58). Single-stranded C-rich circles are considered a specific marker for ALT cells (25) and have been implicated in telomere length extension through the rolling-circle mechanism (9). A ϕ29 DNA polymerase-based assay was developed to detect C-circles in ALT-positive cancer cells (25). In this assay, partially double-stranded C-circles are recognized by ϕ29 DNA polymerase to synthesize a long G-strand DNA, which is generally used as a criterion for the presence of C-circles. To determine whether *RAD27* plays a role in C-circle DNA formation, we established a modified ϕ29 DNA polymerase-based C-circle assay. The ϕ29 DNA polymerase-amplified

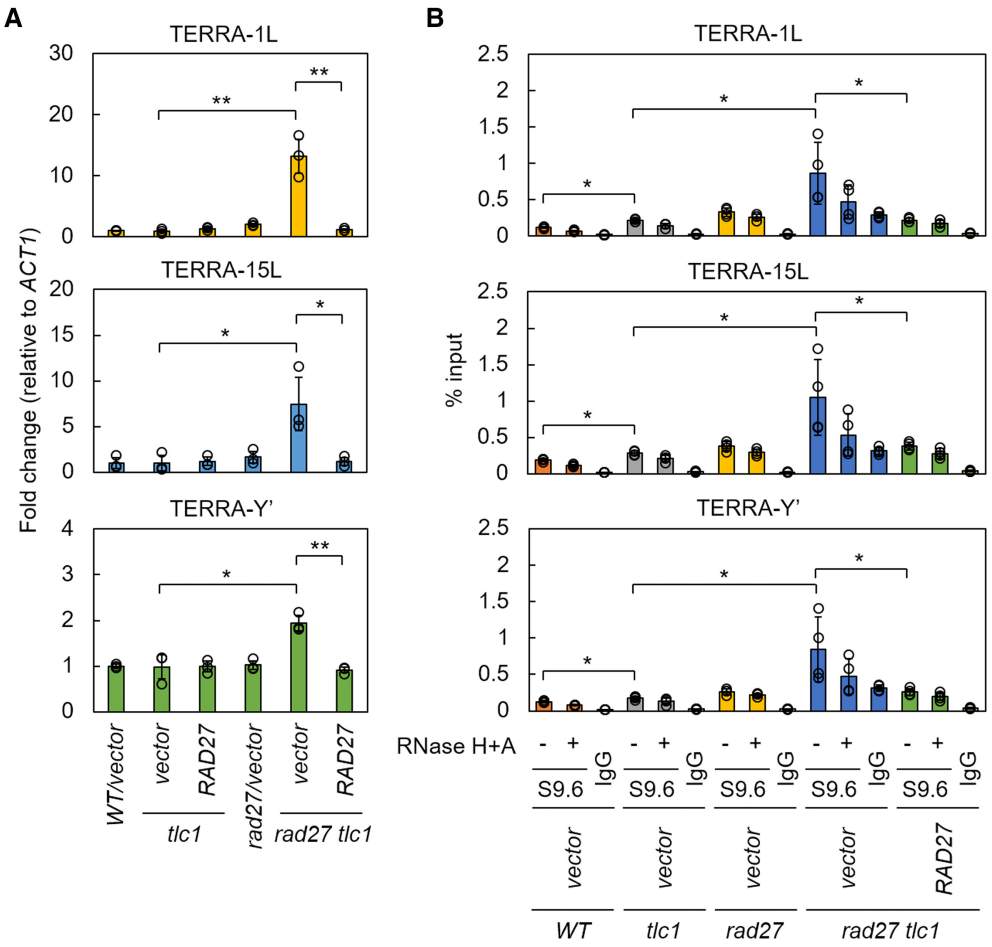

Figure 4. Rad27 suppresses telomere-associated TERRA. (**A**) Rad27 suppresses the TERRA level. Total RNA was extracted from the indicated strains and quantitative RT–PCR analysis was conducted using primer pairs specific for telomere 1L, 15L and Y′-bearing telomeres. The resulting CT values were normalized to *ACT1* RNA levels and presented as relative RNA levels, with the WT value defined as 1. Error bars represent the SD of three independent experiments. *P*-values were determined by a two-tailed paired *t*-test. **P* <0.05. (**B**) Rad27 reduces the level of telomere-associated TERRA. Genomic DNA was extracted from the indicated strains, sonicated and treated with mixtures of RNase H and RNase A. Reaction products were then immunoprecipitated with S9.6 antibody or IgG. The levels of telomere-associated TERRA were quantified as a percentage of the input. *P*-values were determined by a two-tailed unpaired *t*-test. **P* <0.05.

C-circle levels were relatively low in the initial three dilutions of *tlc1* cells (Figure 6A). The C-circle signals peaked at the fourth to fifth dilutions and then gradually decreased. In *rad27 tlc1* cells, the C-circle signals were greatly elevated at the second dilution, sustained at a high level for several dilutions, and then decreased (Figure 6B). Interestingly, detection of C-circle DNA appears to coincide with type II telomere recombination, suggesting a close correlation between C-circles and type II telomere recombination. To test whether introduction of *RAD27* could rescue the elevated C-circle levels in *rad27 tlc1* cells, we introduced a *CEN* plasmid carrying *RAD27* into *rad27 tlc1* cells. As shown in Figure 6C, elevated C-circle levels were suppressed by restoring *RAD27* in *rad27 tlc1* cells, indicating a key role for *RAD27* in regulating C-circle levels. Furthermore, regulation of C-circles by Rad27 is activity dependent, as the Rad27-DA mutant failed to suppress C-circle levels in *rad27 tlc1* cells (Supplementary Figure S7).

DISCUSSION

We found that mutations in*DNA2*, *EXO1*, *MRE11* and *SAE2* delayed type II telomere recombination in yeast. Mre11 is a protein that forms a complex with Rad50 and Xrs2, known as the MRX complex, and is involved in various DNA metabolic processes, including homologous recombination, base-excision repair, double-strand break repair and maintenance of telomeres. The MRX complex, along with Dna2, Exo1 and Sae2, participates in the end resection process during double-strand break repair. This supports the notion that type II telomere recombination is mediated through a similar mechanism. Interestingly, *RAD27* was the only nuclease mutation that caused an early formation of type II survivors, indicating its suppressive role in regulating type II recombination. In *rad27* mutant cells, we found that telomere-associated TERRA was increased, demonstrating the role of *RAD27* in suppressing the accumulation of TERRA on telomeres. Recent studies suggest

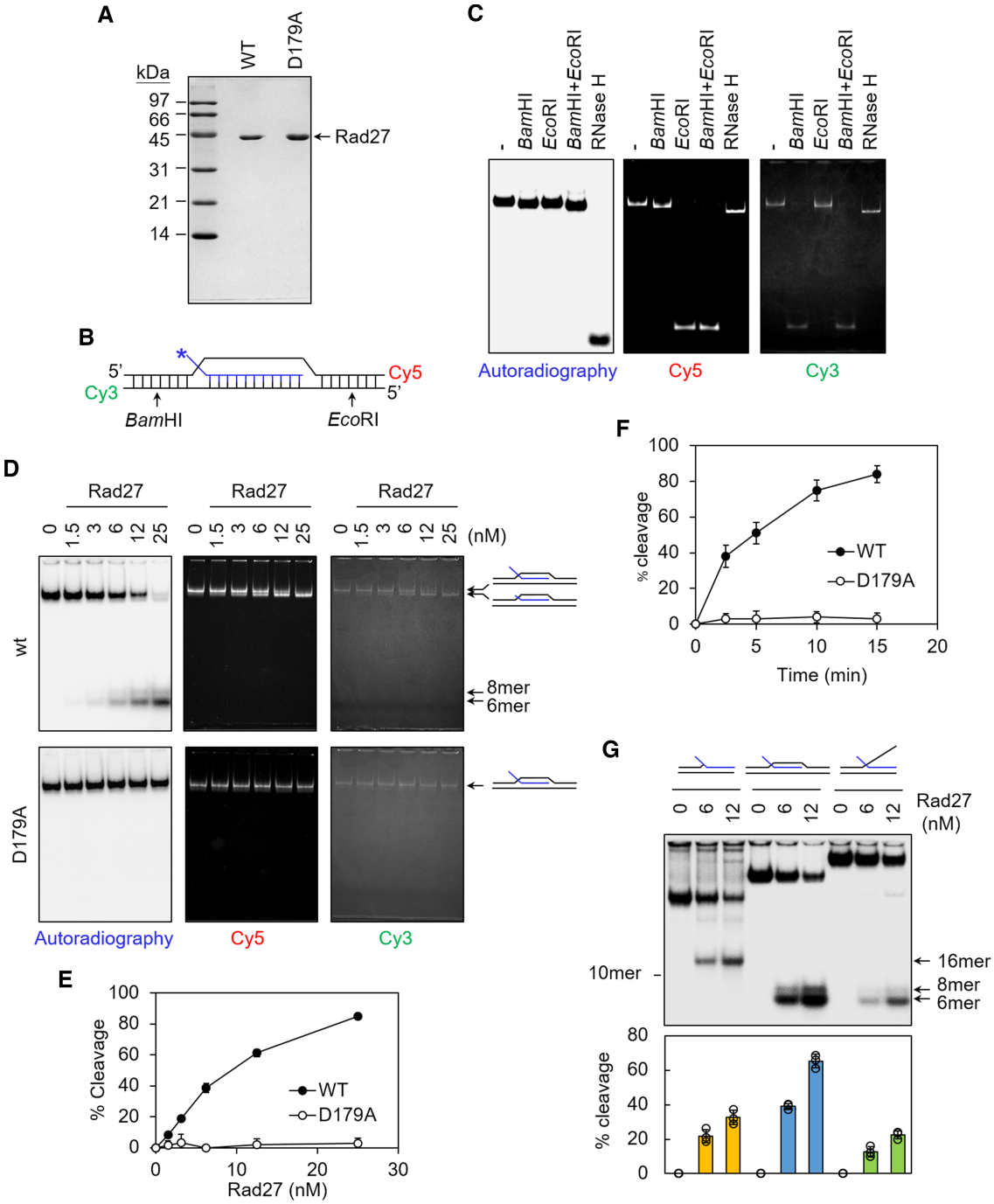

Figure 5. Rad27 selectively cleaves the RNA component of the R-loop structure. (**A**) Rad27 WT or nuclease-dead mutant (D179A) protein was expressed in *E. coli.*, purified and resolved by 15% SDS–PAGE followed by Coomassie blue staining. (**B**) Schematic diagram of the R-loop substrate labeled with isotope ^{32}P on the 5′ end of RNA, and with Cy5 and Cy3 on the top and bottom strands of DNA, respectively. The asterisk denotes the ^{32}P label. Positions of BamHI and EcoRI restriction cutting sites are indicated. (**C**) The R-loop substrate was confirmed by the treatment with BamHI, EcoRI or RNase H. Cleavage of the substrate by BamHI and/or EcoRI confirms the presence of double-stranded DNA (dsDNA) flanking the R-loop. Cleavage by *E. coli.* RNase H confirms the presence of an RNA–DNA hybrid in the R-loop. The radiolabeled or fluorescent signals of the substrates and products were visualized by phosphorimaging and fluorescence imaging, respectively. (**D**) The R-loop substrate (40 nM) was mixed with the indicated amounts of Rad27 WT or D179A and incubated at 30°C for 15 min. Reaction mixtures were resolved on a 10% polyacrylamide gel. Radiolabeled or fluorescent signals of the reaction products were then visualized by phosphorimaging and fluorescence imaging, respectively. (**E**) Quantification of the Rad27 cleavage activity shown in (D). Average values and SDs from three independent experiments are presented. (**F**) The R-loop substrate (40 nM) was incubated with 25 nM each of Rad27 WT or D179A for the indicated times at 30°C. Reaction mixtures were resolved on a 10% polyacrylamide gel. Radiolabeled or fluorescent signals of the substrates and products were then visualized by phosphorimaging and fluorescence imaging, respectively. Average values and SDs from three independent experiments are presented. (**G**) Rad27 prefers to cleave the RNA component of the R-loop structure. The single-flapped (left), R-loop (middle) and double-flapped (left) DNA substrates (40 nM) were incubated with the indicated amounts of Rad27 at 30°C for 15 min and analyzed as above. The autoradiograph of the gel (top) and quantification of the results (bottom) from three independent experiments are presented.

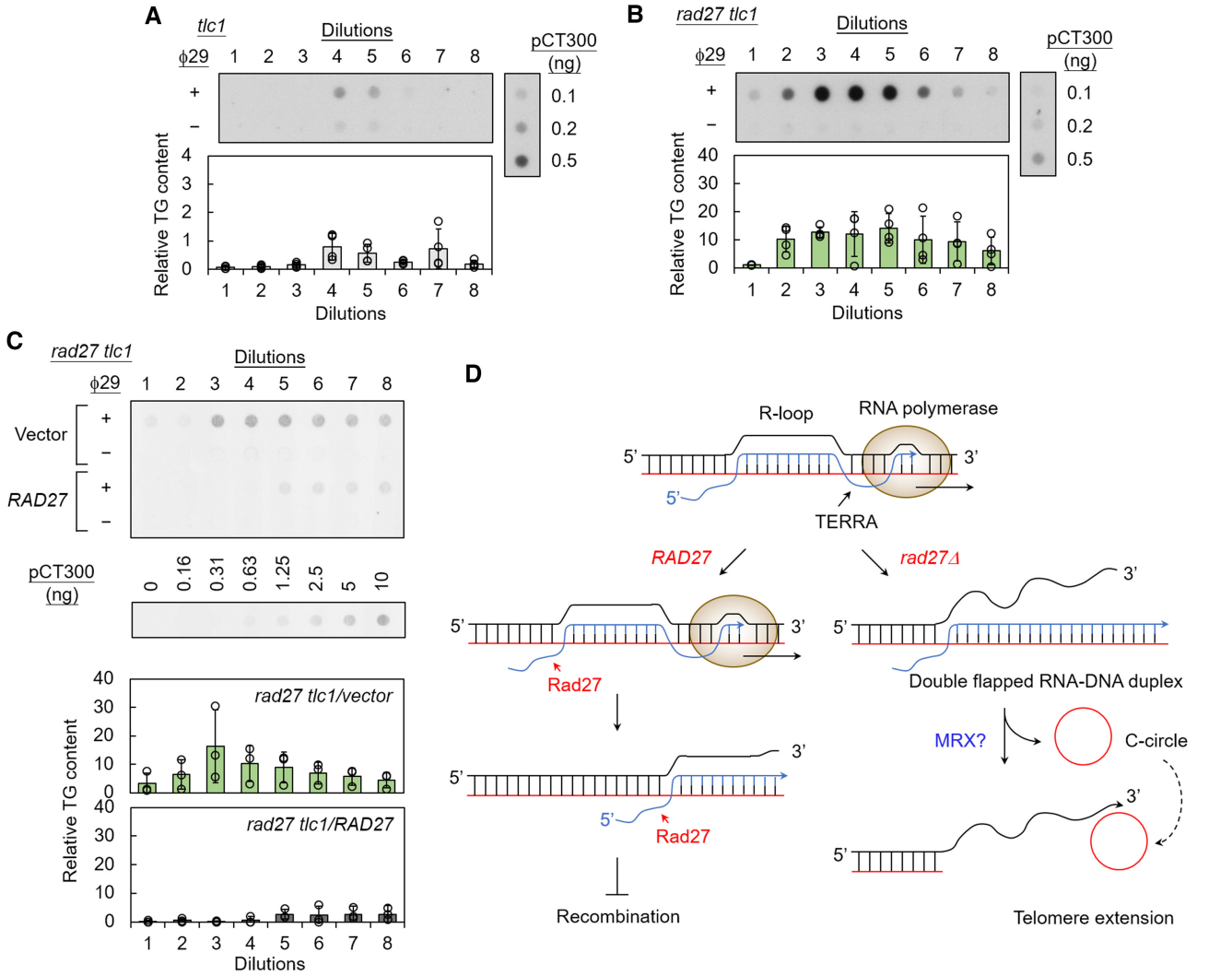

Figure 6. Generation of C-circle DNA in *rad27 tlc1* cells. (**A**) Detection of C-circle DNA during senescence and survivor formation in *tlc1* cells. Genomic DNA was isolated from senescent cultures of *tlc1* cells. A 40 ng aliquot of genomic DNA was subjected to C-circle analysis in the presence or absence of ϕ29 DNA polymerase. Reaction products were spotted onto a nylon membrane and then probed with [γ-^{32}P]ATP-end-labeled $C_{1-3}A$ oligonucleotides. The plasmid pCT300 was used to quantify the relative C-circle signal. Average values and SDs from three independent colonies are presented. (**B**) Elevation of C-circle DNA in *rad27 tlc1* cells. As described above, dot blots and quantification of the C-circle signal in *rad27 tlc1* cells are presented. Average values and SDs were obtained from three independent experiments. (**C**) *RAD27* suppresses formation of C-circle DNA in *tlc1* cells. As described above, C-circle analyses were conducted in *rad27 tlc1* cells expressing *RAD27* or vector. In this experiment, the membrane was probed with Cy5-labeled $C_{1-3}A$ oligonucleotides. Average values and SDs were obtained from three independent colonies. (**D**) Model of the R-loop structure cleaved by Rad27 to inhibit type II recombination formation.

that Rad27 is also involved in R-loop processing (59,60), although the mechanism has not been investigated in detail. Additionally, it has been reported that depletion of human Fen1, the Rad27 equivalent in *S. cerevisiae*, results in RNase H-dependent fragility on the leading strand of telomeres (61). This suggests that Fen1 may process RNA–DNA intermediates generated from co-directional collisions between the replisome and RNA polymerase. These results support the involvement of Rad27 in telomere recombination mediated through the R-loop structure. We also demonstrated that Rad27 cleaves the RNA component of an R-loop molecule, providing direct evidence for its involvement in processing R-loop structures. Furthermore, the finding of Rad27 in suppressing C-circle accumulation may provide a mechanistic link between R-loop structure and C-circles during telomere recombination.

Based on these findings, a model is proposed to describe the suppressive role of Rad27 in restricting type II recombination (Figure 6D). In this model, RNA polymerase transcribes TERRA to form an R-loop structure, which then reaches the end of the DNA to open up a flapped RNA–DNA hybrid structure. In WT cells, Rad27 cleaves TERRA from R-loop or flapped structures using its flap endonuclease activity, thereby preventing DNA breaks and C-circle formation on telomeres. In *rad27* cells, accumulation of the R-loop or flapped RNA–DNA duplex may promote the formation of C-circles. It is worth noting that a recent study revealed that human TERRA could associate with short

telomeres via the formation of R-loop structures that can form *in trans* (62). However, it is unclear whether R-loop formation can occur *in trans* in budding yeast and how Rad27 cleaves TERRA of R-loop *in trans,* which requires further characterization. Since the C-circle structure is considered to be a template for rolling-circle amplification of telomere sequences (9), formation of C-circles could extend telomere sequences. The mechanistic insight of the R-loop structure related to C-circle formation requires further investigation. Additional nucleases and/or DNA processing enzymes may be required to digest R-loop structures and further generate C-circles. Given the involvement of the MRX complex in type II recombination, it is important to determine whether the MRX complex can function on R-loop or double-flapped RNA–DNA structures to facilitate the formation of C-circles.

The formation of R-loop structures during transcription has been shown to have a negative impact on genome stability (63). Therefore, it is crucial to prevent the accumulation of R-loop structure in order to maintain genome integrity. However, only a limited number of protein activities have been reported to regulate the accumulation of R-loop structures. For example, cellular RNase H is known to degrade the RNA component of the RNA–DNA duplex to prevent the formation of the R-loop structure. Furthermore, several helicases that unwind the RNA–DNA duplex have been shown to limit the accumulation of R-loops (28–31). In this study, we have discovered that in addition to its well-known function in Okazaki fragment processing, Rad27 can regulate the R-loop structure. The R-loop processing activity of Rad27 prevents the accumulation of telomere-associated TERRA and C-circle DNA, thereby inhibiting telomere recombination. Although it remains unclear whether the R-loop processing activity of Rad27 is limited to telomeres, based on the preference of Rad27 to process R-loop over double-flapped structures (Figure 5), it is likely that Rad27 also participates in limiting the accumulation of R-loop structures within chromosomes to maintain genome stability.

The interference with RNA polymerase elongation activity has been closely linked to the formation of R-loop structures. For example, stalled RNA polymerase has been shown to promote the formation of R-loop structures (64). Conversely, R-loop structures have been reported to interfere with RNA polymerase elongation (65). Thus, although R-loop structures formed by TERRA are considered factors in regulating telomere recombination, it is also possible that stalled RNA polymerase might contribute to telomere recombination. In yeast, the average size of TERRA is ∼380 bases (51), and the transcription elongation rate of RNA polymerase II is ∼12–30 bases/s (66,67). The average period for an RNA polymerase to stay on a telomere template is <30 s, so the RNA polymerase might quickly run off the telomere template after transcription. Indeed, chromatin immunoprecipitation analysis fails to identify resident RNA polymerase on telomeres during telomere recombination (Supplementary Figure S8). Alternatively, we found that disruption of R-loop structures by either RNase H, helicases or topoisomerase impacts telomere recombination. We also provide direct evidence for the processing of the R-loop structure by Rad27. For these reasons, we exclude the possibility that stalled RNA polymerase is involved in inducing telomere recombination. Collectively, the R-loop or double-flap RNA–DNA duplex structures formed by TERRA are more likely to be critical for telomere recombination than RNA polymerase.

It has been demonstrated that human Fen1 substrates adopt a double-flap structure with a characteristic 1 nt 3′ flap (40,53). Crystal structure analyses have revealed a closed chamber in Fen1 that accommodates the 3′ flap and binds to a 1 nt 3′ overhang, while also binding to the 5′ flap through the formation of a hydrophobic wedge around the 3′ flap (68). This conformation orients the Fen1 nuclease activity to the base of the flap, leading to cleavage near the point where the 5′ flap is annealed to the template strand (40,68). In our study, we have shown that Rad27 prefers to cleave R-loops over the single- or double-flap substrates. Using the same oligonucleotide sequences, Rad 27 generates a 16 nt product on the short 1 nt double-flap substrate, while producing products with 6 and 8 nt upon cleavage of R-loop and long double-flap structures (Figure 5G). Hence, Rad27 may employ a distinct mechanism for the recognition and cleavage of R-loop and long double-flap structures. Further structural analysis is required to gain mechanistic insights into the contribution of the RNA component and/or a long 5′ flap to this unique cleavage pattern of Rad27 on R-loop substrates.

In yeast, Mus81 and Yen1 are the two well-characterized enzymes that are involved in resolving Holliday junctions (20,69), a key intermediate generated during the final stage of DNA recombination. In this study, we found that mutations in *mus81* or *yen1* did not affect telomere recombination, although disruption of both activities significantly reduced cell viability. Interestingly, type II survivors eventually formed in senescent *mus81 yen1 tlc1* cells (Figure 2F), suggesting that an alternative mechanism that does not require Holliday junction resolvase activity might be utilized for type II telomere recombination. Previous studies have reported that mammalian and *Drosophila* homologs of topoisomerase IIIα and BLM helicase possess Holliday junction processing activity *in vitro* (70,71). Given that the yeast *TOP3*/*SGS1* has been shown to be important for type II recombination (72), it is possible that the Holliday junctions formed near telomeres are resolved by the unwinding activity of *TOP3*/*SGS1* during recombination.

Dna2 is a helicase that function in a 5′ to 3′ direction and has specificity for forked DNA substrates (48,49). In addition to its helicase activity, it also possesses both 5′- to 3′- and 3′- to 5′-exo/endonuclease activities (73,74). The role of Dna2 in telomere recombination had been investigated. Studies have shown that double mutants carrying the *dna2-2* mutation, which affects the helicase domain (R1235Q) (75), and the telomerase mutants senesce more rapidly than single telomerase mutants (76). Type II survivors arise more rapidly in double mutants than in single telomerase mutants (76), indicating that Dna2 helicase activity is involved in suppressing type II telomere recombination. In this study, we found that the *dna2-1 tlc1* cells are sick, senesce early and no type II survivor is detected (Figure 1C; Supplementary Figure S9). The *dna2-1* mutant is a temperature-sensitive mutant and has a mutation in the nuclease domain (P504S), which exhibits greatly reduced nuclease activity of

the Dna2 protein (73). These results suggest that Dna2 has dual roles in regulating telomere recombination, with its helicase activity involved in suppressing telomere recombination and nuclease activity required for type II recombination. Although the exact reason is unclear, it is possible that the apparently opposing functions of Dna2 are regulated by its interaction proteins. For example, Dna2 is known to interact with Mre11 (77), Rad27 (44,78), Rfa1/Rfa2 (79) and Sgs1 (80), which act positively or negatively in regulating telomere recombination. Therefore, specific interactions between Dna2 and its interacting proteins might modulate Dna2 activity to regulate telomere recombination. Investigating how Dna2 coordinates with these proteins to regulate telomere recombination could clarify this issue.

DATA AVAILABILITY

Data on which this article is based are available in the article and in its supplementary online data.

SUPPLEMENTARY DATA

Supplementary Data are available at NAR Online.

ACKNOWLEDGEMENTS

We would like to thank Dr S.C. Teng for his assistance in preparing the manuscript. We also thank Ms Y.C. Tu for critical reading of the manuscript. We thank Dr C.K. Tseng for sharing Typhoon 5 equipment, and the staff of the Taiwan Yeast Bio-resource Center at the First Core Labs, National Taiwan University College of Medicine, for bio-resources sharing.

Author contributions: C.-C. Liu conducted the experiments presented in Figures 1, 3, 4 and 6; H.-R. Chan conducted the experiments presented in Figures 1, 3 and 4; G.-C. Su and K.-H. Lei conducted the experiments presented in Figure 5; Y.-Z. Hsieh conducted the experiments presented in Figure 2; C.-C. Liu, H.-R. Chan, T. Kato and Y.-Z. Hsieh participated in screening of nuclease mutants; T.-Y. Yu and Y.-W. Kao conducted the experiments presented in Figure 1B; T.-H. Cheng provided plasmids used in Figure 1A, discussion and editing the manuscript; P. Chi and J.-J. Lin supervised the project and writing of the manuscript.

FUNDING

This work was supported by the National Taiwan University [Aim for Top University Project 104R8955-2 and 108L9014 to J.-J.L., and NTU Core Consortiums NTU-CC-108L892004 to P.C.] and the Ministry of Science and Technology [MOST107-2311-B-002-023-MY3 and MOST109-2311-B-002-014 to J.-J.L. and MOST 111-2326-B-002-019 and MOST 111-2311-B-002-006-MY3 to P.C.].

Conflict of interest statement. None declared.

REFERENCES

1. Blackburn,E.H. and Collins,K. (2011) Telomerase: an RNP enzyme synthesizes DNA. *Cold Spring Harb. Perspect. Biol.*, **3**, a003558.
2. Sobinoff,A.P. and Pickett,H.A. (2017) Alternative lengthening of telomeres: DNA repair pathways converge. *Trends Genet.*, **33**, 921–932.
3. Singer,M.S. and Gottschling,D.E. (1994) *TLC1*: template RNA component of *Saccharomyces cerevisiae* telomerase. *Science*, **266**, 404–409.
4. Lundblad,V. and Szostak,J.W. (1989) A mutant with a defect in telomere elongation leads to senescence in yeast. *Cell*, **57**, 633–643.
5. Lundblad,V. and Blackburn,E.H. (1993) An alternative pathway for yeast telomere maintenance rescues *est*$^-$ senescence. *Cell*, **73**, 347–360.
6. Le,S., Moore,J.K., Haber,J.E. and Greider,C.W. (1999) *RAD50* and *RAD51* define two pathways that collaborate to maintain telomeres in the absence of telomerase. *Genetics*, **152**, 143–152.
7. Teng,S.-C. and Zakian,V.A. (1999) Telomere–telomere recombination is an efficient bypass pathway for telomere maintenance in *Saccharomyces cerevisiae*. *Mol. Cell. Biol.*, **19**, 8083–8093.
8. Chen,Q., Ijpma,A. and Greider,C.W. (2001) Two survivor pathways that allow growth in the absence of telomerase are generated by distinct telomere recombination events. *Mol. Cell. Biol.*, **21**, 1819–1827.
9. Cesare,A.J. and Reddel,R.R. (2010) Alternative lengthening of telomeres: models, mechanisms and implications. *Nat. Rev. Genet.*, **11**, 319–330.
10. Teng,S.-C., Chang,J., McCowan,B. and Zakian,V.A. (2000) Telomerase-independent lengthening of yeast telomeres occurs by an abrupt Rad50p-dependent, Rif-inhibited recombinational process. *Mol. Cell*, **6**, 947–952.
11. Hu,Y., Tang,H.B., Liu,N.N., Tong,X.J., Dang,W., Duan,Y.M., Fu,X.H., Zhang,Y., Peng,J., Meng,F.L. *et al.* (2013) Telomerase-null survivor screening identifies novel telomere recombination regulators. *PLoS Genet.*, **9**, e1003208.
12. Yu,T.-Y., Kao,Y.-w. and Lin,J.-J. (2014) Telomeric transcripts stimulate telomere recombination to suppress senescence in cells lacking telomerase. *Proc. Natl Acad. Sci. USA*, **111**, 3377–3382.
13. Rippe,K. and Luke,B. (2015) TERRA and the state of the telomere. *Nat. Struct. Mol. Biol.*, **22**, 853–858.
14. Balk,B., Maicher,A., Dees,M., Klermund,J., Luke-Glaser,S., Bender,K. and Luke,B. (2013) Telomeric RNA–DNA hybrids affect telomere-length dynamics and senescence. *Nat. Struct. Mol. Biol.*, **20**, 1199–1205.
15. Graf,M., Bonetti,D., Lockhart,A., Serhal,K., Kellner,V., Maicher,A., Jolivet,P., Teixeira,M.T. and Luke,B. (2017) Telomere length determines TERRA and R-loop regulation through the cell cycle. *Cell*, **170**, 72–85.
16. Sollier,J., Stork,C.T., García-Rubio,M.L., Paulsen,R.D., Aguilera,A. and Cimprich,K.A. (2014) Transcription-coupled nucleotide excision repair factors promote R-loop-induced genome instability. *Mol. Cell*, **56**, 777–785.
17. Yasuhara,T., Kato,R., Hagiwara,Y., Shiotani,B., Yamauchi,M., Nakada,S., Shibata,A. and Miyagawa,K. (2018) Human Rad52 promotes XPG-mediated R-loop processing to initiate transcription-associated homologous recombination repair. *Cell*, **175**, 558–570.
18. Tumbale,P., Williams,J.S., Schellenberg,M.J., Kunkel,T.A. and Williams,R.S. (2014) Aprataxin resolves adenylated RNA–DNA junctions to maintain genome integrity. *Nature*, **506**, 111–115.
19. Sobinoff,A.P., Allen,J.A.M., Neumann,A.A., Yang,S.F., Walsh,M.E., Henson,J.D., Reddel,R.R. and Pickett,H.A. (2017) BLM and SLX4 play opposing roles in recombination-dependent replication at human telomeres. *EMBO J.*, **36**, 2907–2919.
20. Ip,S.C., Rass,U., Blanco,M.G., Flynn,H.R., Skehel,J.M. and West,S.C. (2008) Identification of Holliday junction resolvases from humans and yeast. *Nature*, **456**, 357–361.
21. Tay,Y.D. and Wu,L. (2010) Overlapping roles for Yen1 and Mus81 in cellular Holliday junction processing. *J. Biol. Chem.*, **285**, 11427–11432.
22. Blanco,M.G., Matos,J., Rass,U., Ip,S.C.Y. and West,S.C. (2010) Functional overlap between the structure-specific nucleases Yen1 and Mus81–Mms4 for DNA-damage repair in *S. cerevisiae*. *DNA Repair (Amst.)*, **9**, 394–402.
23. Gietz,R.D. and Schiestl,R.H. (2007) High-efficiency yeast transformation using the LiAc/SS carrier DNA/PEG method. *Nat. Protocols*, **2**, 31–34.

24. Munashingha,P.R., Lee,C.H., Kang,Y.H., Shin,Y.K., Nguyen,T.A. and Seo,Y.S. (2012) The trans-autostimulatory activity of Rad27 suppresses *dna2* defects in Okazaki fragment processing. *J. Biol. Chem.*, **287**, 8675–8687.
25. Henson,J.D., Cao,Y., Huschtscha,L.I., Chang,A.C., Au,A.Y., Pickett,H.A. and Reddel,R.R. (2009) DNA C-circles are specific and quantifiable markers of alternative-lengthening-of-telomeres activity. *Nat. Biotechnol.*, **27**, 1181–1185.
26. Pfeiffer,V., Crittin,J., Grolimund,L. and Lingner,J. (2013) The THO complex component Thp2 counteracts telomeric R-loops and telomere shortening. *EMBO J.*, **32**, 2861–2871.
27. El Hage,A., French,S.L., Beyer,A.L. and Tollervey,D. (2010) Loss of topoisomerase I leads to R-loop-mediated transcriptional blocks during ribosomal RNA synthesis. *Genes Dev.*, **24**, 1546–1558.
28. Steinmetz,E.J., Conrad,N.K., Brow,D.A. and Corden,J.L. (2001) RNA-binding protein Nrd1 directs poly(A)-independent 3′-end formation of RNA polymerase II transcripts. *Nature*, **413**, 327–331.
29. Martin-Tumasz,S. and Brow,D.A. (2015) *Saccharomyces cerevisiae* Sen1 helicase domain exhibits 5′- to 3′-helicase activity with a preference for translocation on DNA rather than RNA. *J. Biol. Chem.*, **290**, 22880–22889.
30. Boule,J.-B. and Zakian,V.A. (2007) The yeast Pif1p DNA helicase preferentially unwinds RNA–DNA substrates. *Nucleic Acids Res.*, **35**, 5809–5818.
31. Chib,S., Byrd,A.K. and Randey,K. (2016) Yeast helicase Pif1 unwinds RNA:DNA hybrids with higher processivity than DNA:DNA duplexes. *J. Biol. Chem.*, **291**, 5889–5901.
32. Boule,J.-B., Vega,L.R. and Zakian,V.A. (2005) The yeast Pif1p helicase removes telomerase from telomeric DNA. *Nature*, **438**, 57–61.
33. Bertuch,A.A. and Lundblad,V. (2004) *EXO1* contributes to telomere maintenance in both telomerase-proficient and telomerase-deficient *Saccharomyces cerevisiae*. *Genetics*, **166**, 1651–1659.
34. Joseph,I.S., Kumari,A., Bhattacharyya,M.K., Gao,H., Li,B. and Lustig,A.J. (2010) An mre11 mutation that promotes telomere recombination and an efficient bypass of senescence. *Genetics*, **185**, 761–770.
35. Maringele,L. and Lydall,D. (2004) *EXO1* plays a role in generating type I and type II survivors in budding yeast. *Genetics*, **166**, 1641–1649.
36. Guh,C.-Y., Shen,H.-J., Chen,L.W., Chiu,P.-C., Liao,I.-H., Lo,C.-C., Chen,Y., Hsieh,Y.-H., Chang,T.-C., Yen,C.-P. *et al.* (2022) XPF activates break-induced telomere synthesis. *Nat. Commun.*, **13**, 5781.
37. Mullen,J.R., Kaliraman,V., Ibrahim,S.S. and Brill,S.J. (2001) Requirement for three novel protein complexes in the absence of the Sgs1 DNA helicase in *Saccharomyces cerevisiae*. *Genetics*, **157**, 103–118.
38. Fricke,W.M. and Brill,S.J. (2003) Slx1-Slx4 is a second structure-specific endonuclease functionally redundant with Sgs1-Top3. *Genes and Develop*, **17**, 1768–1778.
39. Harrington,J.J. and Lieber,M.R. (1994) Functional domains within *FEN-1* and *RAD2* define a family of structure-specific endonucleases: implications for nucleotide excision repair. *Genes Dev.*, **8**, 1344–1355.
40. Balakrishnan,L. and Bambara,R.A. (2013) Flap endonuclease 1. *Annu. Rev. Biochem.*, **82**, 119–138.
41. Ghaemmaghami,S., Huh,W.-K., Bower,K., Howson,R.W., Belle,A., Dephoure,N., O'Shea,E.K. and Weissman,J.S. (2003) Global analysis of protein expression in yeast. *Nature*, **425**, 737–741.
42. Kulak,N.A., Pichler,G., Paron,I., Nagaraj,N. and Mann,M. (2014) Minimal, encapsulated proteomic-sample processing applied to copy-number estimation in eukaryotic cells. *Nat. Methods*, **11**, 319–324.
43. Tishkoff,D.X., Boerger,A.L., Bertrand,P., Filosi,N., Gaida,G.M., Kane,M.F. and Kolodner,R.D. (1997) Identification and characterization of *Saccharomyces cerevisiae EXO1*, a gene encoding an exonuclease that interacts with *MSH2*. *Proc. Natl Acad. Sci. USA*, **94**, 7487–7492.
44. Budd,M.E. and Campbell,J.L. (1997) A yeast replicative helicase, Dna2 helicase, interacts with yeast FEN-1 nuclease in carrying out its essential function. *Mol. Cell. Biol.*, **17**, 2136–2142.
45. Jin,Y.H., Ayyagari,R., Resnick,M.A., Gordenin,D.A. and Burgers,P.M.J. (2003) Okazaki fragment maturation in yeast. II. Cooperation between the polymerase and 3′–5′-exonuclease activities of Pol delta in the creation of a ligatable nick. *J. Biol. Chem.*, **278**, 1626–1633.
46. Fiorentini,P., Huang,K.N., Tishkoff,D.X., Kolodner,R.D. and Symington,L.S. (1997) Exonuclease I of *Saccharomyces cerevisiae* functions in mitotic recombination *in vivo* and *in vitro*. *Mol. Cell. Biol.*, **17**, 2764–2773.
47. Tran,P.T., Erdeniz,N., Dudley,S. and Liskay,R.M. (2002) Characterization of nuclease-dependent functions of Exo1p in *Saccharomyces cerevisiae*. *DNA Repair (Amst.)*, **1**, 895–912.
48. Budd,M.E. and Campbell,J.L. (1995) A yeast gene required for DNA replication encodes a protein with homology to DNA helicases. *Proc. Natl Acad. Sci. USA*, **92**, 7642–7646.
49. Budd,M.E., Choe,W.-C. and Campbell,J.L. (1995) *DNA2* encodes a DNA helicase essential for replication of eukaryotic chromosomes. *J. Biol. Chem.*, **270**, 26766–26769.
50. Bae,S.H. and Seo,Y.S. (2000) Characterization of the enzymatic properties of the yeast Dna2 helicase/endonuclease suggests a new model for Okazaki fragment processing. *J. Biol. Chem.*, **275**, 38022–38031.
51. Luke,B., Panza,A., Redon,S., Iglesias,N., Li,Z. and Lingner,J. (2008) The Rat1p 5′ to 3′ exonuclease degrades telomeric repeat-containing RNA and promotes telomere elongation in *Saccharomyces cerevisiae*. *Mol. Cell*, **32**, 465–477.
52. Boguslawski,S.J., Smith,D.E., Michalak,M.A., Mickelson,K.E., Yehle,C.O., Patterson,W.L. and Carrico,R.J. (1986) Characterization of monoclonal antibody to DNA·RNA and its application to immunodetection of hybrids. *J. Immunol. Methods*, **89**, 123–130.
53. Kao,H.-I., Henricksen,L.A., Liu,Y. and Bambara,R.A. (2002) Cleavage specificity of *Saccharomyces cerevisiae* flap endonuclease 1 suggests a double-flap structure as the cellular substrate. *J. Biol. Chem.*, **277**, 14379–14389.
54. Bryan,T.M., Englezou,A., Gupta,J., Bacchetti,S. and Reddel,R.R. (1995) Telomere elongation in immortal human cells without detectable telomerase activity. *EMBO J.*, **14**, 4240–4248.
55. Cesare,A.J. and Griffith,J.D. (2004) Telomeric DNA in ALT cells is characterized by free telomeric circles and heterogeneous T-loops. *Mol. Cell. Biol.*, **24**, 9948–9957.
56. Wang,R.C., Smogorzewska,A. and de Lange,T. (2004) Homologous recombination generates T-loop-sized deletions at human telomeres. *Cell*, **119**, 355–368.
57. Nabetani,A. and Ishikawa,F. (2009) Unusual telomeric DNAs in human telomerase-negative immortalized cells. *Mol. Cell Biol.*, **29**, 703–713.
58. Lin,C.Y., Chang,H.H., Wu,K.J., Tseng,S.F., Lin,C.C., Lin,C.P. and Teng,S.C. (2005) Extrachromosomal telomeric circles contribute to Rad52-, Rad50-, and polymerase δ-mediated telomere–telomere recombination in *Saccharomyces cerevisiae*. *Eukaryot. Cell*, **4**, 327–336.
59. Chang,E.Y., Tsai,S., Aristizabal,M.J., Wells,J.P., Coulombe,Y., Busatto,F.F., Chan,Y.A., Kumar,A., Dan Zhu,Y., Wang,A.Y. *et al.* (2019) MRE11–RAD50–NBS1 promotes Fanconi Anemia R-loop suppression at transcription–replication conflicts. *Nat. Commun.*, **10**, 4265.
60. Cristini,A., Ricci,G., Britton,S., Salimbeni,S., Huang,S.N., Marinello,J., Calsou,P., Pommier,Y., Favre,G., Capranico,G. *et al.* (2019) Dual processing of R-loops and topoisomerase I induces transcription-dependent DNA double-strand breaks. *Cell Rep.*, **28**, 3167–3181.
61. Teasley,D.C., Parajuli,S., Nguyen,M., Moore,H.R., Alspach,E., Lock,Y.J., Honaker,Y., Saharia,A., Piwnica-Worms,H. and Stewart,S.A. (2015) Flap endonuclease 1 limits telomere fragility on the leading strand. *J. Biol. Chem.*, **290**, 15133–15145.
62. Feretzaki,M., Pospisilova,M., Fernandes,R.V., Lunardi,T., Krejci,L. and Lingner,J. (2020) RAD51-dependent recruitment of TERRA lncRNA to telomeres through R-loops*Nature*, **587**, 303–308.
63. Santos-Pereira,J.M. and Aguilera,A. (2015) R loops: new modulators of genome dynamics and function. *Nat. Rev. Genet.*, **16**, 583–597.
64. Zhang,X., Chiang,H.-C., Wang,Y., Zhang,C., Smith,S., Zhao,X., Nair,S.J., Michalek,J., Jatoi,I., Lautner,M. *et al.* (2017) Attenuation of RNA polymerase II pausing mitigates BRCA1-associated R-loop accumulation and tumorigenesis. *Nat. Commun.*, **8**, 15908.
65. Belotserkovskii,B.P. and Hanawalt,P.C. (2011) Anchoring nascent RNA to the DNA template could interfere with transcription. *Biophys. J.*, **100**, 675–684.

66. Kaplan,C.D., Jin,H., Zhang,I.L. and Belyanin,A. (2012) Dissection of Pol II trigger loop function and Pol II activity-dependent control of start site selection *in vivo*. *PLoS Genet.*, **8**, e1002627.
67. Mason,P.B. and Struhl,K. (2005) Distinction and relationship between elongation rate and processivity of RNA polymerase II *in vivo*. *Mol. Cell*, **17**, 831–840.
68. Chapados,B.R., Hosfield,D.J., Han,S., Qiu,J., Yelent,B., Shen,B. and Tainer,J.A. (2004) Structural basis for FEN-1 substrate specificity and PCNA-mediated activation in DNA replication and repair. *Cell*, **116**, 39–50.
69. Boddy,M.N., Gaillard,P.H., McDonald,W.H., Shanahan,P., Yates,J.R. and Russell,P. (2001) Mus81–Eme1 are essential components of a Holliday junction resolvase. *Cell*, **107**, 537–548.
70. Plank,J.L., Wu,J. and Hsieh,T.-s. (2006) Topoisomerase IIIα and Bloom's helicase can resolve a mobile double Holliday junction substrate through convergent branch migration. *Proc. Natl Acad. Sci. USA*, **103**, 11118–11123.
71. Bussen,W., Raynard,S., Busygina,V., Singh,A.K. and Sung,P. (2007) Holliday junction processing activity of the BLM–Topo IIIα–BLAP75 complex. *J. Biol. Chem.*, **282**, 31484–31492.
72. Tsai,H.-J., Huang,W.-H., Li,T.-K., Tsai,Y.-L., Wu,K.-J., Tseng,S.-F. and Teng,S.-C. (2006) Involvement of topoisomerase III in telomere–telomere recombination. *J. Biol. Chem.*, **281**, 13717–13723.
73. Budd,M.E., Choe,W.-C. and Campbell,J.L. (2000) The nuclease activity of the yeast DNA2 protein, which is related to the RecB-like nucleases, is essential *in vivo*. *J. Biol. Chem.*, **275**, 16518–16529.
74. Lee,K.-H., Kim,D.W., Bae,S.-H., Kim,J.-A., Ryu,G.-H., Kwon,Y.-N., Kim,K.-A., Koo,H.-S. and Seo,Y.-S. (2000) The endonuclease activity of the yeast Dna2 enzyme is essential *in vivo*. *Nucleic Acids Res.*, **28**, 2873–2881.
75. Formosa,T. and Nittis,T. (1999) DNA2 mutants reveal interactions with DNA polymerase α and CTF4, a Pol α accessory factor, and show that full DNA2 helicase activity is not essential for growth. *Genetics*, **151**, 1459–1470.
76. Choe,W., Budd,M., Imamura,O., Hoopes,L. and Campbell,J.L. (2002) Dynamic localization of an Okazaki fragment processing protein suggests a novel role in telomere replication. *Mol. Cell. Biol.*, **22**, 4202–4217.
77. Niu,H., Chung,W.-H., Zhu,Z., Kwon,Y., Zhao,W., Chi,P., Prakash,R., Seong,C., Liu,D., Lu,L. *et al.* (2010) Mechanism of the ATP-dependent DNA end-resection machinery from *Saccharomyces cerevisiae*. *Nature*, **467**, 108–111.
78. Henry,R.A., Balakrishnan,L., Ying-Lin,S.T., Campbell,J.L. and Bambara,R.A. (2010) Components of the secondary pathway stimulate the primary pathway of eukaryotic Okazaki fragment processing. *J. Biol. Chem.*, **285**, 28496–28505.
79. Bae,K.H., Kim,H.S., Bae,S.H., Kang,H.Y., Brill,S. and Seo,Y.S. (2003) Bimodal interaction between replication-protein A and Dna2 is critical for Dna2 function both *in vivo* and *in vitro*. *Nucleic Acids Res.*, **31**, 3006–3015.
80. Cejka,P., Cannavo,E., Polaczek,P., Masuda-Sasa,T., Pokharel,S., Campbell,J.L. and Kowalczykowski,S.C. (2010) DNA end resection by Dna2-Sgs1-RPA and its stimulation by Top3-Rmi1 and Mre11-Rad50-Xrs2. *Nature*, **467**, 112–116.
81. Saharia,A. and Stewart,S.A. (2009) FEN1 contributes to telomere stability in ALT-positive tumor cells. *Oncogene*, **28**, 1162–1167.